

## Supporting Information

# Activation and Assembly of Plasmonic-Magnetic Nanosurfactants for Encapsulation and Triggered Release

*Fei Liu,<sup>†</sup> Yifan Li,<sup>†</sup> Yanhua Huang,<sup>†</sup> Ayuna Tsyrenova,<sup>†</sup> Kyle Miller,<sup>†</sup> Lin Zhou,<sup>†,§</sup> Hantang  
Qin,<sup>‡</sup> Shan Jiang<sup>†,‡,§,\*</sup>*

<sup>†</sup>Department of Materials Science and Engineering and <sup>‡</sup>Department of Industrial and  
Manufacturing Systems Engineering, Iowa State University, Ames, Iowa 50011, United States

<sup>§</sup>Division of Materials Science and Engineering, Ames Laboratory, Ames, Iowa 50011, United  
States

## Materials and Methods

*Chemicals:* Gold(III) chloride trihydrate ( $\text{HAuCl}_4 \cdot 3\text{H}_2\text{O}$ ,  $\geq 99.9\%$  trace metals basis), oleylamine (OAm, 70%), borane tert-butylamine complex (97%), 1-octadecene (ODE, 90%), iron pentacarbonyl ( $\text{Fe}(\text{CO})_5$ ,  $\geq 99.99\%$  trace metals basis), oleic acid (OA, 90%), 3,4-dihydroxybenzoic acid ( $\geq 97\%$ ), thiol-terminated polystyrene ( $M_n$  11,000,  $\text{PDI} \leq 1.1$ ), were purchased from Sigma-Aldrich. All solvents were obtained from Sigma-Aldrich. CdSe quantum dots were purchased from NNCrystal US Corporation. Milli-Q water with a resistivity  $>18.0 \text{ M}\Omega \cdot \text{cm}$  was used in the preparation of aqueous solutions.

*Preparation of Au-Fe<sub>3</sub>O<sub>4</sub> nanosurfactants:* Au-Fe<sub>3</sub>O<sub>4</sub> dumbbell-like nanoparticles were synthesized according to our previous work.<sup>1</sup> An acid treatment was then applied to activate the surface of as-prepared Au-Fe<sub>3</sub>O<sub>4</sub> nanoparticles. Typically, Au-Fe<sub>3</sub>O<sub>4</sub> nanoparticles (15 mg) were dispersed in toluene (5 ml) and acetone (5 ml). Subsequently, 0.5 ml  $\text{HNO}_3$  (70%) was added to the solution. The product was then collected by centrifugation (5,000 rpm, 1 min) and further dispersed in toluene (5 ml) containing 0.1 ml oleylamine. The above acid treatment was applied once again, and the product was dispersed in toluene.

Surface modification by ligand exchange was carried out to make amphiphilic Au-Fe<sub>3</sub>O<sub>4</sub> nanoparticles as nanosurfactants. For typical surface modification, Au-Fe<sub>3</sub>O<sub>4</sub> nanoparticles were first modified with polystyrene by mixing nanoparticles (15 mg) with thiol-terminated polystyrene (20 mg) in toluene (5 ml). The mixture was stirred for 24 h, and nanoparticles were washed by toluene/acetone solution three times. Then, nanoparticles were mixed with 3,4-dihydroxybenzoic acid in tetrahydrofuran (THF, 1 ml, 50 mg/ml) under sonication. Acetone was added to the above mixture solutions to precipitate the nanoparticles. The Au-Fe<sub>3</sub>O<sub>4</sub> nanosurfactants were further dispersed in the desired solvents for different purposes.

*Preparation of superstructures of Au-Fe<sub>3</sub>O<sub>4</sub> nanosurfactants:* The emulsions stabilized by nanosurfactants were first prepared. The nanosurfactants (0.5 mg) were dispersed in the toluene/DMF (0.5 ml/0.1 ml) solution by sonication. Then 0.1 ml of NaOH solution (0.5 M) was added, and the mixture was agitated by a vortex mixer for 20 s. The nanosurfactants were separated by centrifugation at 10,000 rpm for 1 min, and the solvents in the supernatant were discarded. To prepare the oil-in-water emulsion, the precipitated nanosurfactants were mixed with the oil (e.g., toluene, 0.1 ml) and water (0.5 ml), and the mixture was agitated by a vortex mixer for 20 s. The water-in-oil emulsion was prepared in a similar way, except that the oil (e.g., toluene, 0.5 ml) and water (0.1 ml) were used. The superstructures were prepared from self-assembly of nanosurfactants by collapsing different emulsions. The toluene-in-water emulsion stabilized by nanosurfactants was used to fabricate clusters with hydrophilic lobe facing outward while hydrophobic lobe staying close. The as-prepared emulsion was sonicated for 30 min, and the product was separated and further purified with DI water three times by using centrifugation. For inverse clusters, the water-in-toluene emulsion was used. DMF (0.1 ml) was added into the emulsion, and the mixture was sonicated for 30 min. The product was separated and further purified with toluene three times by using centrifugation. The superstructures are reversible between clusters and inverse clusters by changing the solvents. For example, toluene containing 20% v/v DMF was used to replace water to prepare inverse clusters. The solution was sonicated for 20 min, and the product was washed by toluene three times. Inverse clusters suspended in toluene were reversed by changing the solvent from toluene to water. The solution was sonicated for 10 min, and the product was washed by water three times.

*Nanoparticles (CdSe QDs, Au, Fe<sub>3</sub>O<sub>4</sub>, Fe nanoparticles) encapsulation:* Hydrophobic nanoparticles were purchased or synthesized according to the literature.<sup>2-4</sup> The chloroform-in-

water emulsion was prepared with hydrophobic nanoparticles dispersed in chloroform (0.1 mg/ml) based on the method described in the previous sections. A solution of NaOH (0.1 M) was added to adjust the pH of the water to ~10. Then 0.1 ml DMF was added, and the mixture was agitated by a vortex mixer for 20 s and further sonicated by 20 min. The product was collected and washed by water three times.

*Small molecules (pyrene, Nile red, DOX) encapsulation and release:* The toluene-in-water emulsion was prepared with small molecules dispersed in toluene (0.5 mg/ml) based on the method described in the previous sections. The emulsion was sonicated for 30 min, and the product was separated and further purified with DI water three times by using centrifugation. The release of pyrene was studied by shaking the sample solution (1 ml) at 500 rpm for different periods of time. At each time point, the solution was centrifuged at 5,000 rpm, and 100  $\mu$ l supernatant was collected. Fresh water was added to compensate for the volume loss of the solution. The collected supernatant was mixed with 300  $\mu$ L dimethyl sulfoxide (DMSO) in a black 96-well plate. A standard curve was made through a serial dilution. Fluorescence of the pyrene was measured using a plate reader (BioTek Synergy HT Multidetector Microplate Reader) at an excitation/emission of 360/460 nm. For the laser triggered pyrene release, at the time points of 2 h, 6 h and 12 h, an optical-fiber-coupled diode laser with wavelengths of 808 nm and power intensity of 0.8 W/cm<sup>2</sup> was employed for 5 min. After irradiating, the released pyrene was collected and measured by using a plate reader. The release of Nile red was triggered by adding 5% v/v DMF into the solution. 20  $\mu$ l of the solution was dropped onto a glass slide and imaged by an optical fluorescent microscope (Leica DMI8). The release of DOX was triggered by adjusting the pH of the solution. The pH was adjusted to ~4 by a solution of HCl (1M). After

that, 20  $\mu$ l of the solution was dropped onto a glass slide and imaged by an optical fluorescent microscope (Leica DMI8).

*Characterization:* A JEOL 2100 scanning/transmission electron microscope (STEM) operating at 200 kV was used to acquire bright-field transmission electron microscopy images. Aberration-corrected high angle annular dark field scanning transmission electron microscopy (HAADF-STEM) images were acquired on a Titan Themis 300 probe corrected TEM. Energy-dispersive X-ray spectroscopy (EDS) was acquired on a Tecnai G2-F20 microscope equipped with an EDX detector. Scanning electron microscopy (SEM) images were acquired on a scanning electron microscope (FEI Quanta 250) at an accelerating voltage of 10 kV. The oil-in-water and water-in-oil emulsions stabilized by Au-Fe<sub>3</sub>O<sub>4</sub> nanosurfactants were imaged by an optical fluorescent microscope (Leica DMI8). Encapsulation of CdSe QDs by Au-Fe<sub>3</sub>O<sub>4</sub> nanosurfactants was imaged using Zeiss 780 confocal microscope with an excitation wavelength of 561 nm. UV-Vis absorption spectra were measured on an Agilent Cary 60 UV-Vis spectrophotometer. The atomic force microscopy images were acquired on a Bruker Dimension Icon AFM in Tapping Mode. Captured Images were plain fit to remove sample tilt and analyzed using average height cross-sections to determine feature height relative to substrate background. The interfacial tension between water and toluene in the presence of nanosurfactants was measured using pendant drop tensiometry. A drop of water containing nanosurfactants was injected into toluene. The interfacial tension was acquired by fitting the axisymmetric profile of the droplet to the Young-Laplace equation.

### **Synthesis, activation, and functionalization of Au-Fe<sub>3</sub>O<sub>4</sub> nanoparticles.**

Au-Fe<sub>3</sub>O<sub>4</sub> dumbbell-like nanoparticles were first synthesized as the core component for the fabrication of nanosurfactants based on a previously reported seeded-growth method.<sup>1</sup> To ensure

reproducible surface properties, an essential post-treatment with acid was developed to thoroughly clean and activate the as-synthesized nanoparticles before further surface functionalization. The rationale of this additional activation process is to effectively remove the iron species (e.g., iron oxide island/layer) deposited on the Au lobe during secondary lobe growth. Even though no additional structure is visible on the Au lobe surface under high-resolution electron microscope (Figure S1), atomic level deposition of other species may prevent the Au lobe from being completely functionalized.

After the acid cleansing treatment, these nano-dumbbells were further modified asymmetrically to generate their amphiphilicity. Previous studies demonstrated the functionalization of Au-Fe<sub>3</sub>O<sub>4</sub> nanoparticles with thiolated and catecholic molecules, with the thiol attaching to Au and the catechol attaching to Fe<sub>3</sub>O<sub>4</sub>, respectively.<sup>5-6</sup> Here, for the hydrophobic side, the Au lobe was originally covered by pristine oleylamine, which can be further enhanced with a bulkier and more stable polymeric ligand thiol-terminated polystyrene ( $M_n$ , 11,000 g/mol). The strong thiolate-gold bond ensures stable functionalization on the Au lobe. For the hydrophilic side, the Fe<sub>3</sub>O<sub>4</sub> lobe was functionalized with catechol derivatives. For example, carboxylic groups can be tethered to the hydrophilic lobe through a ligand exchange with 3,4-dihydroxybenzoic acid. Although catechol moiety would also interact with the Au surface, the catechol adsorption on Au could be minimized by the two-step selective functionalization due to the protection of polystyrene layer.<sup>7</sup> To further prove it, we examined the stability of thiol-terminated polystyrene on Au against catechol modification. Polystyrene functionalized Au nanoparticles were treated with 3,4-dihydroxybenzoic acid under the same ligand exchange condition for Au-Fe<sub>3</sub>O<sub>4</sub> nano-dumbbells. The treated Au nanoparticles could not be dispersed in water but were easily

dispersed in organic solvents such as toluene, indicating limited adsorption of catechol moiety on Au.

### **Assembly of Au-Fe<sub>3</sub>O<sub>4</sub> nanosurfactants.**

The configurations of nanosurfactant structures clearly resemble the micelle and inverse micelle structures formed by small surfactant molecules, even though the detailed interactions among nanosurfactants are significantly different from molecular surfactants. This means the principles guiding the orientation and assembly of small surfactant molecules also apply to nanosurfactants. Although micelle and inverse micelle structures are common with surfactant molecules, similar structures formed by nanosurfactants are not trivial considering strong VDW forces often lead to irreversible aggregation of nanoparticles. Here, VDW forces are strong enough to secure the nanosurfactant adsorbed at emulsion interface into free-standing clusters and lock the orientation from being carried away during the evaporation. VDW forces did not stop nanosurfactants from detaching and re-assembling when emulsions were renewed. The reversibility has the important implication that nanosurfactants can be responsive to the change of the environment, cycle through different phases, and re-establish the structures dynamically.

### **Emulsion stabilization by nanosurfactants.**

Nanosurfactants with different Janus balance and packing parameters (Figure 3) have the tendency to adsorb at the oil-water interface to stabilize Pickering emulsions. It was suggested that a higher packing parameter resulting from a higher Janus balance would lead nanoparticle surfactants to curve towards the aqueous phase.<sup>8-9</sup> As a result, the formation of water-in-oil Pickering emulsion was more desirable, especially when Janus balance was high.<sup>9</sup> Although all

of our nanosurfactants could stabilize both oil-in-water and water-in-oil emulsions, the water-in-oil emulsion showed much better stability, which is consistent with previous studies.<sup>9</sup>

### Supplementary Figures

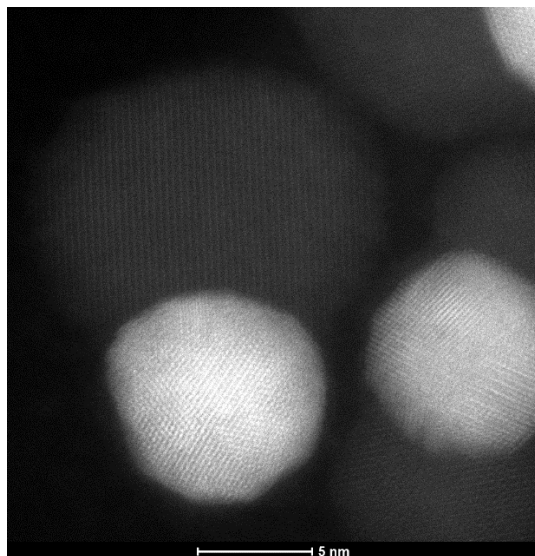


Figure S1. HAADF-STEM image of a typical Au-Fe<sub>3</sub>O<sub>4</sub> nanocrystal.

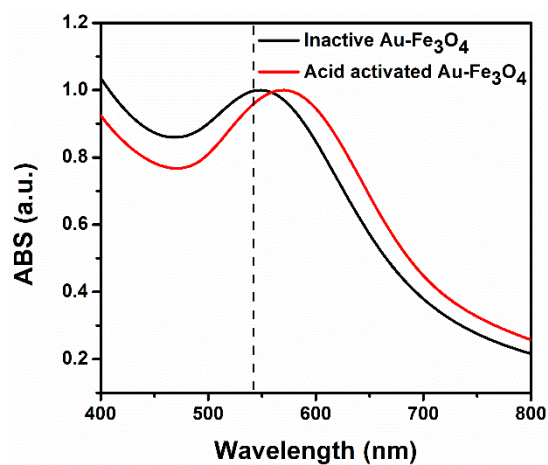


Figure S2. UV-vis spectra of structures assembled from inactive and acid-activated Au-Fe<sub>3</sub>O<sub>4</sub> nanoparticles. The dashed line indicates the absorption peak of un-assembled Au-Fe<sub>3</sub>O<sub>4</sub> nanoparticles.



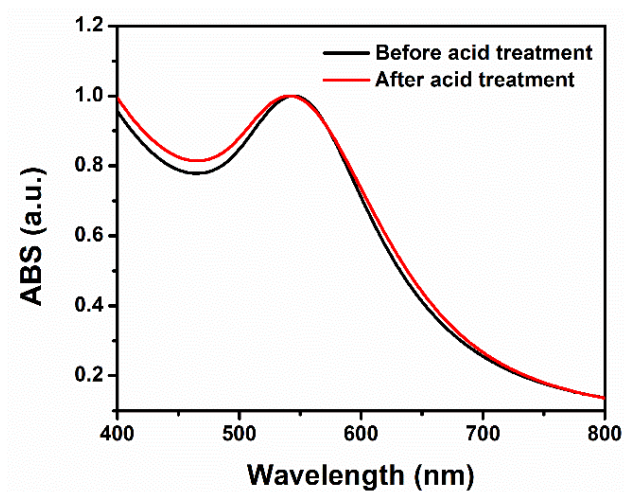


Figure S3. UV-vis spectra of homogenous Au-Fe<sub>3</sub>O<sub>4</sub> nanoparticles before and after acid treatment.

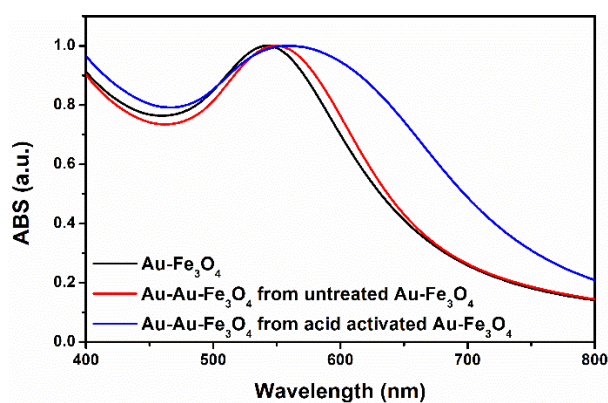


Figure S4. UV-vis spectra of Au-Fe<sub>3</sub>O<sub>4</sub> nanoparticles and Au-Au-Fe<sub>3</sub>O<sub>4</sub> obtained from Au-Fe<sub>3</sub>O<sub>4</sub> before and after acid treatment.

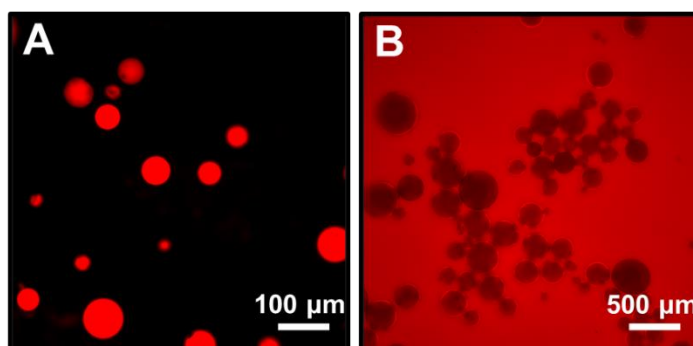


Figure S5. Fluorescent microscope images of (A) toluene-in-water emulsion and (B) water-in-toluene emulsion with the toluene phase labelled by Nile red.



Figure S6. Optical images of dispersed Au-Fe<sub>3</sub>O<sub>4</sub> nano-dumbbells in the solution in the absence and presence of an external magnet for 5 min.

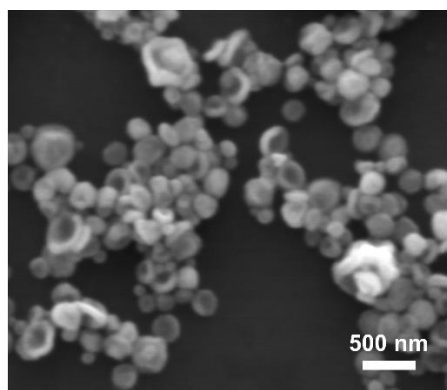


Figure S7. SEM image of structures assembled from Au-Fe<sub>3</sub>O<sub>4</sub> nanosurfactants with Janus balance of 0.79.

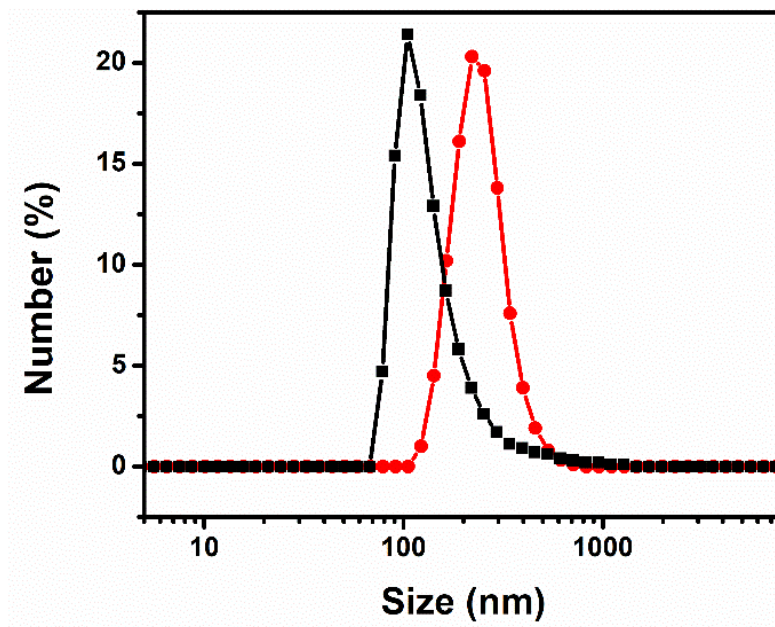


Figure S8. Hydrodynamic diameter distribution of capsules from self-assembly of Au-Fe<sub>3</sub>O<sub>4</sub> nanosurfactants with Janus balance of 0.59 (black line) and 0.79 (red line).

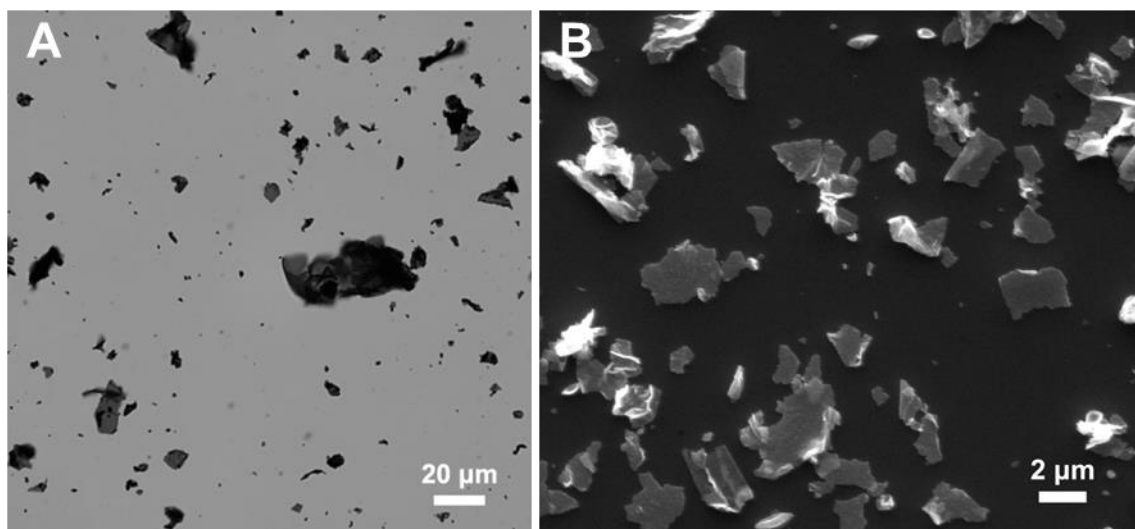


Figure S9. (A) Optical microscopy image and (B) SEM image of sheets from self-assembly of Au-Fe<sub>3</sub>O<sub>4</sub> nanosurfactants with Janus balance of 0.92.

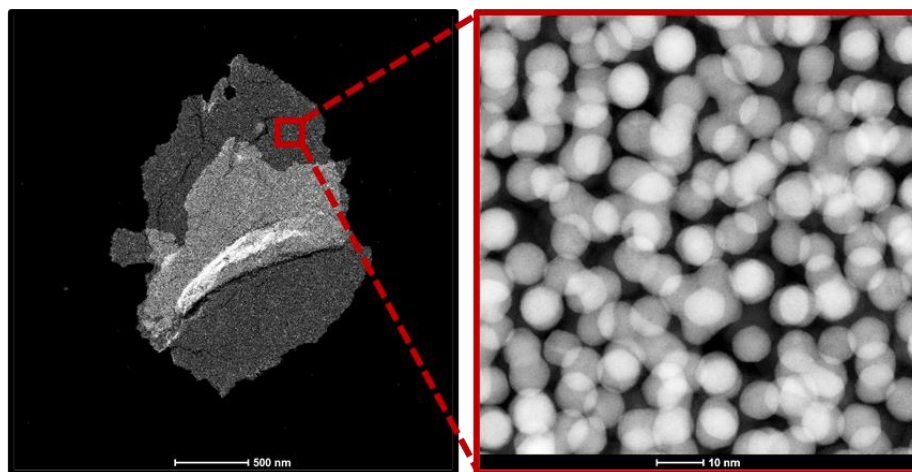


Figure S10. HAADF-STEM images of sheets from self-assembly of Au-Fe<sub>3</sub>O<sub>4</sub> nanosurfactants at different magnifications.

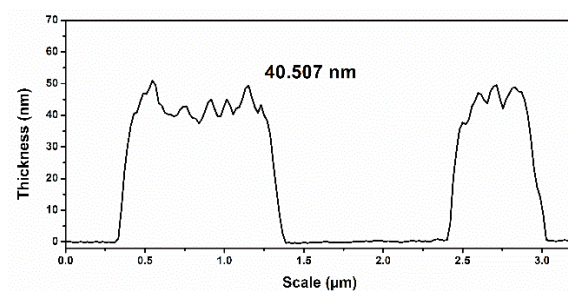
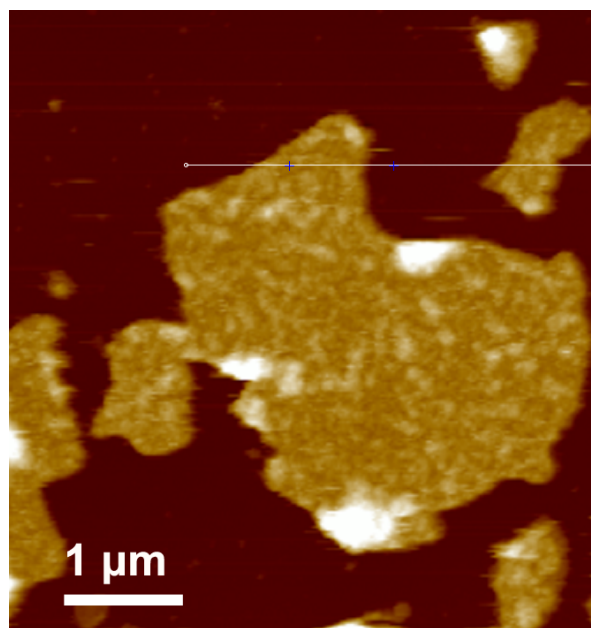




Figure S11. AFM image of sheets from self-assembly of Au-Fe<sub>3</sub>O<sub>4</sub> nanosurfactants with Janus balance of 0.92.

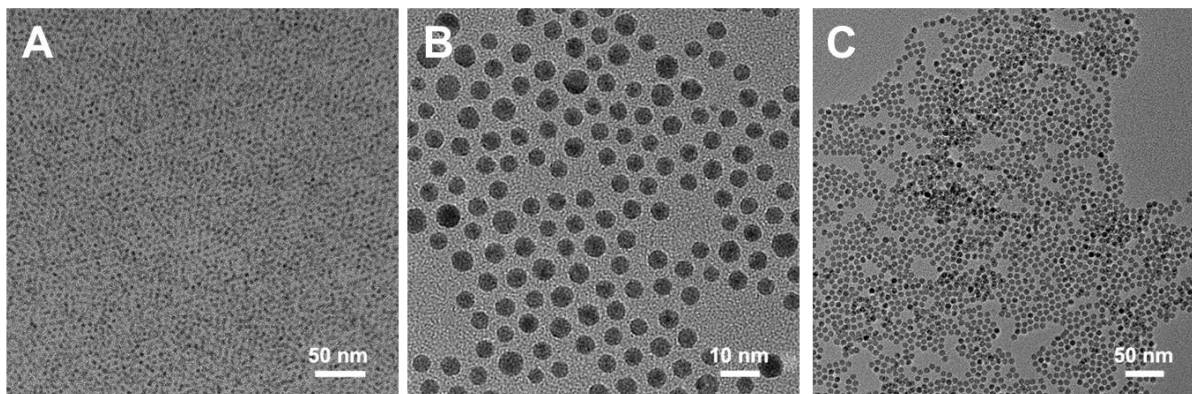


Figure S12. TEM images of (A) octadecylamine coated CdSe QDs, (B) oleylamine coated Au nanoparticles, and (C) oleic acid coated Fe<sub>3</sub>O<sub>4</sub> nanoparticles.

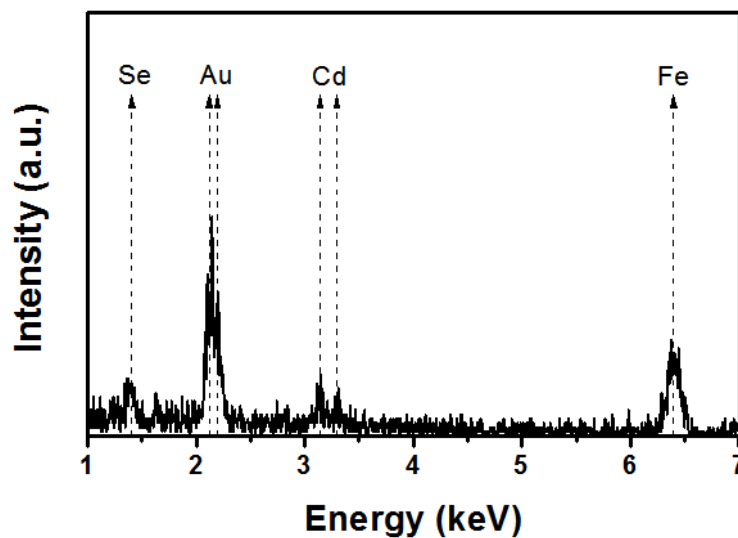


Figure S13. EDS spectrum of nanosurfactants encapsulating QDs.

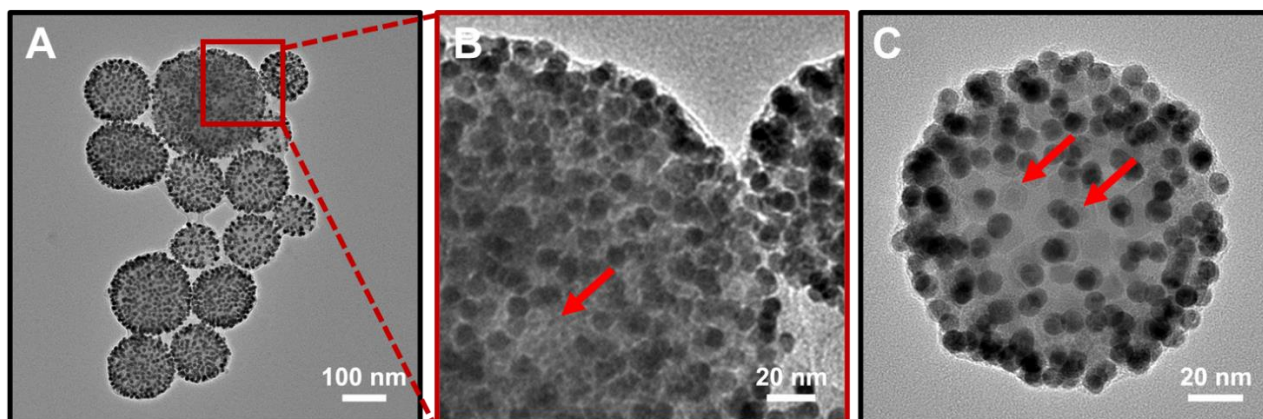


Figure S14. TEM images of the encapsulation of (A, B) CdSe QDs and (C) Fe nanoparticles by nanosurfactants when water-in-oil emulsion was utilized. Arrows indicate the positions of encapsulated nanoparticles.

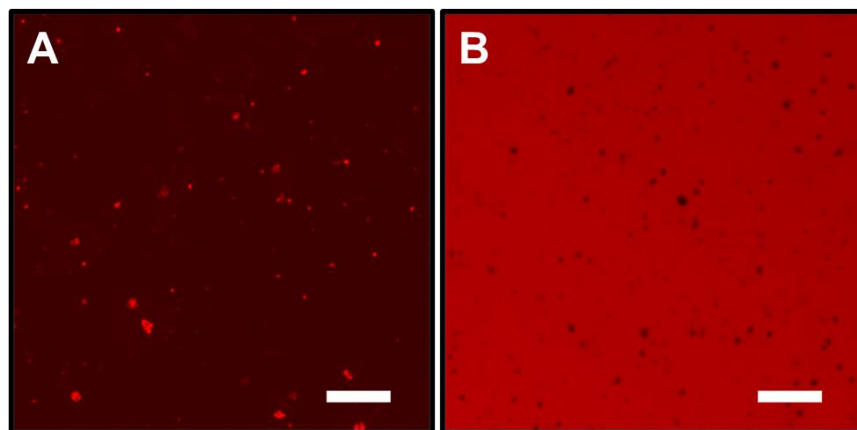


Figure S15. Fluorescent images showing hydrophilic DOX A) encapsulation and B) triggered release by changing the solvent from toluene to water. Scale bar, 20  $\mu\text{m}$ .

## Reference

1. Liu, F.; Goyal, S.; Forrester, M.; Ma, T.; Miller, K.; Mansoorieh, Y.; Henjum, J.; Zhou, L.; Cochran, E.; Jiang, S., Self-assembly of Janus Dumbbell Nanocrystals and Their Enhanced Surface Plasmon Resonance. *Nano Lett.* **2019**, *19* (3), 1587-1594.
2. Peng, S.; Wang, C.; Xie, J.; Sun, S., Synthesis and Stabilization of Monodisperse Fe Nanoparticles. *J. Am. Chem. Soc.* **2006**, *128* (33), 10676-10677.
3. Peng, S.; Lee, Y.; Wang, C.; Yin, H.; Dai, S.; Sun, S., A facile synthesis of monodisperse Au nanoparticles and their catalysis of CO oxidation. *Nano Res.* **2008**, *1* (3), 229-234.
4. Park, J.; An, K.; Hwang, Y.; Park, J.-G.; Noh, H.-J.; Kim, J.-Y.; Park, J.-H.; Hwang, N.-M.; Hyeon, T., Ultra-large-scale syntheses of monodisperse nanocrystals. *Nat. Mater.* **2004**, *3* (12), 891-895.
5. Xu, C.; Xie, J.; Ho, D.; Wang, C.; Kohler, N.; Walsh, E. G.; Morgan, J. R.; Chin, Y. E.; Sun, S., Au–Fe<sub>3</sub>O<sub>4</sub> Dumbbell Nanoparticles as Dual-Functional Probes. *Angew. Chem. Int. Ed.* **2008**, *47* (1), 173-176.
6. Xu, C.; Wang, B.; Sun, S., Dumbbell-like Au–Fe<sub>3</sub>O<sub>4</sub> Nanoparticles for Target-Specific Platin Delivery. *J. Am. Chem. Soc.* **2009**, *131* (12), 4216-4217.
7. Klinkova, A.; Thérien-Aubin, H.; Choueiri, R. M.; Rubinstein, M.; Kumacheva, E., Colloidal analogs of molecular chain stoppers. *Proc. Natl. Acad. Sci. U. S. A.* **2013**, *110* (47), 18775.
8. Aveyard, R.; Binks, B. P.; Clint, J. H., Emulsions stabilised solely by colloidal particles. *Adv. Colloid Interface Sci.* **2003**, *100-102*, 503-546.
9. Xie, S.; Chen, S.; Zhu, Q.; Li, X.; Wang, D.; Shen, S.; Jin, M.; Zhou, G.; Zhu, Y.; Shui, L., Janus Nanoparticles with Tunable Amphiphilicity for Stabilizing Pickering-Emulsion Droplets via Assembly Behavior at Oil–Water Interfaces. *ACS Appl. Mater. Interfaces* **2020**, *12* (23), 26374-26383.